Bulletin de la Société Royale des Sciences de Liège, Vol. 80, 2011, p. 410 - 414

Escaping Radiation from Massive Star H II regions in the Magellanic Clouds

E.W. Pellegrini[1], M.S. Oey[1], P.F. Winkler[2], R.C. Smith[3] and S. Points[3]

[1] Department of Astronomy, University of Michigan, 500 Church St., Ann Arbor, MI, USA
[2] Department of Physics, Middlebury College, Middlebury, VT, USA
[3] CTIO, Casilla 603, La Serena, Chile

Abstract: We present a novel approach for distinguishing density-bounded vs radiation bounded H II regions based on [S II]/Hα and [S II]/[O III] ratio maps. We find most H II regions fall into one of three categories: radiation bounded, open blister type, and density bounded. Our approach directly diagnoses the existence of ionization fronts around massive stars, revealing a significant number of H II regions to be density bounded. Furthermore, we can place a lower limit on the fraction of ionizing photons escaping each region yielding values consistent with other methods, with direct implications for the ionization of the Warm Interstellar Medium and reionization of the universe at high redshift. We conclude that the three morphological classifications are correlated with the observed N(H I) column density and Hα luminosity, however a more filamentary structure of the LMC does not lead to higher H II escape fractions than in the SMC.

1 Introduction

It is critical that we determine the fate of ionizing radiation generated by massive stars. The optical depth to ionizing radiation, τ, and the fraction of ionizing radiation not immediately absorbed by H II regions, $f_{\rm esc} \equiv e^{-\tau}$, are of great importance to many fields of astrophysics, including the epoch of reionization. During this period bright quasars were less frequent than now, and alone were insufficient to reionize the universe (Sokasian, Abel & Hernquist 2003). If $f_{\rm esc}$ was large, young star forming galaxies would have generated enough ionizing radiation to make up the difference and ionize the universe by $z \sim 6$. A significant $f_{\rm esc}$ from H II regions will also have implications on the origin of the large scale, diffuse Warm Ionized Medium (WIM) of galaxies (Haffner et al. 2009), and derivations of star formation rates, stellar populations and IMF of high redshift galaxies using Hα observations. Therefore the value of $f_{\rm esc}$, and its dependence on environment is a fundamental parameter that must be better constrained.

Unfortunately, determining $f_{\rm esc}$ for individual H II regions is quite difficult, requiring indirect methods often with inconclusive results ranging between zero to unity. Giammanco et al. (2004) demonstrated that emission line ratios alone cannot differentiate between a density bounded (DB) or radiation bounded (RB) H II region in the case where the nebulae contain optically thick clumps. In their models, radiation escapes along low density lines of sight, free of clumps, resulting in a large

$f_{\rm esc}$. However, the spectrum is dominated by the high density clumps, each forming an individual ionization front (IF) with a spectrum similar to constant density RB models. A more promising approach to constrain $f_{\rm esc}$ relates the observed H II region Hα luminosity, L(Hα), to the expected rate of H ionizing photons (Q(H)) from a stellar population. Any discrepancy between the expected and observed L(Hα) is attributed to a non-zero value of $f_{\rm esc}$. With this method, uncertainties in Q(H) as large as a factor of 2, translate to values of $f_{\rm esc}$ ranging between 0 and 50%.

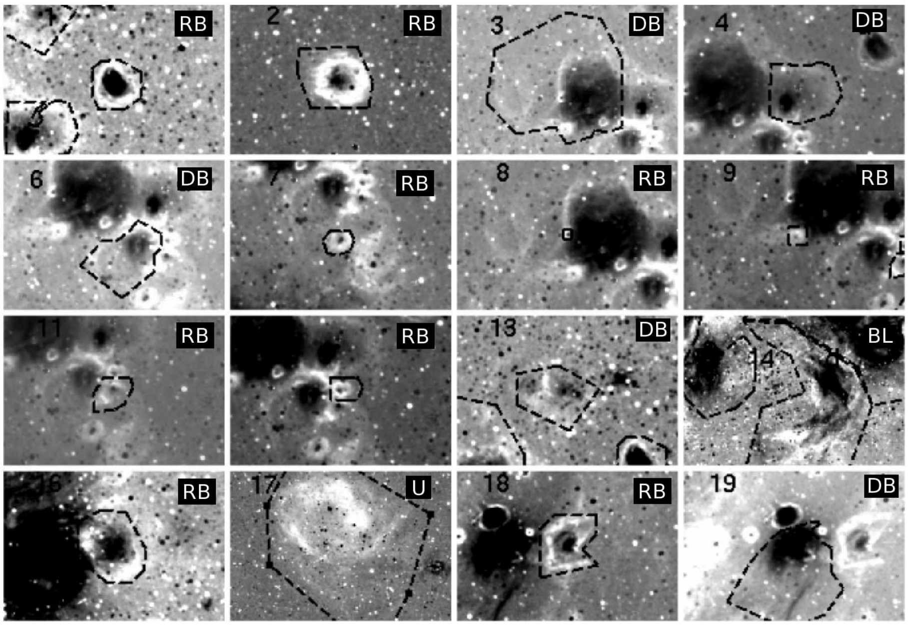

Figure 1: A sample of LMC H II regions from the MCELS survey as seen in [S II]/[O III]. The dashed contours represent the boundary of the aperture used to measure Hα fluxes and H I column densities. In the upper right corner of each individual panel the morphology of the object is indicated as RB, DB, BL or U (unknown).

2 Differentiating Radiation and Density Bounded Nebulae

To make progress in this important field we detect IFs unique to RB nebulae with [S II]/Hα and [S II]/[O III] ratio maps of the LMC and SMC which trace changes in gas ionization. For individual H II regions, seen in Figure 1, the different ionization potentials of S^0, H^0 and O^+ result in IFs appearing as limb-brightened [S II] enhancements (white). IFs in RB H II regions surround both the ionizing stars and the ionized gas (weak [S II]; black). In comparison, the DB H II regions are characterized by highly ionized gas with no surrounding IF, signaling a high $f_{\rm esc}$.

This method allows nearly all known H II regions in both the LMC and SMC to be separated into one of 3 empirically motivated categories: RB, DB or Blister type (BL) nebulae. BL type regions have IFs with only a partial covering factor, allowing radiation to escape the region in only certain directions. Using emission lines this way avoids many of the uncertainties inherent in previous studies.

We use data from the Magellanic Cloud Emission Line Survey (MCELS, Smith et al. 2005). Over 5 years, the MCELS collaboration obtained deep emission line images covering most of the LMC and SMC in Hα, [O III] and [S II] with a resolution of 5 arcsec. This survey was intended to provide data useful for research into the ionized gas of these galaxies. The data are ideal for our study because they are homogeneous and complete down to $L(\mathrm{H}\alpha) \simeq 10^{35}\ \mathrm{erg\ s^{-1}}$, which includes all known H II regions in both galaxies. We use these data to define a new set of physically motivated boundaries for a complete sample of all H II regions in both galaxies. These boundaries are also used for our Hα photometry apertures. In some cases we find nebulae previously identified as distinct to be part of a larger single structure. In addition, some newly identified nebulae are detected within larger complexes.

3 Escape Fraction of Ionizing Radiation

We seek a diagnostic to quantize the global $f_{\rm esc}$, but the relative strengths of the emission lines we use depend on more parameters than just the local depth to ionizing radiation. These include the effective temperature of the ionizing stars $T_{\rm eff}$, and the ionization parameter U, defined as ratio of ionizing photon flux to hydrogen density. To constrain the possible values of $f_{\rm esc}$, we have used CLOUDY (Ferland et al. 1998) to simulate H II regions over a large range of $T_{\rm eff}$, U and $f_{\rm esc}$ characteristic of nebulae ionized by O-stars. Using 2D projections of the predicted surface brightness of emission lines we are able to make direct comparisons to our ionization maps. We find a general trend that the [S II] enhancement used to identify IFs at the edges of RB H II regions is absent in DB H II if $f_{\rm esc} \geq 0.6$. This also means that H II regions with signatures of an IF may have $f_{\rm esc}$ as large as 0.6, depending on $T_{\rm eff}$ and U.

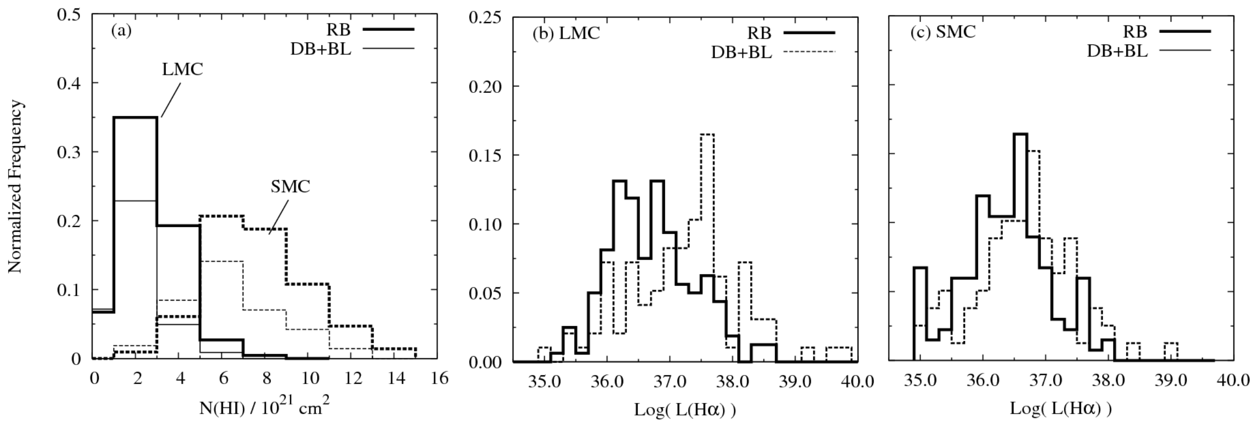

Figure 2: a) Distribution of N(H I) measured within the projected aperture used for the Hα photometry. RB(thick line) and DB+BL(thin) objects in both the LMC(solid) and SMC(dashed) are normalized by the total number of objects in each category; b) the LMC L(Hα) distribution with the same line types used in (a); c) same as plot (b) for the SMC.

To derive a global escape fraction from the entire H II region population, we first sum the observed H II region $L_{\rm H\,II}({\rm H}\alpha)$, proportional to $Q({\rm H})_{\rm absorbed}$. Then we estimate the rate of *ionizing* radiation escaping into and ionizing the WIM ($Q({\rm H})_{\rm esc}$) from $L_{esc}({\rm H}\alpha) = L_{\rm H\,II}({\rm H}\alpha) \times (f_{\rm esc}/(1-f_{\rm esc}))$, where $L_{esc}({\rm H}\alpha)$ is the Hα luminosity resulting from $Q({\rm H})_{\rm esc}$. Our simulations constrain RB regions to $f_{esc}({\rm RB}) \leq 0.6$ and DB to $0.6 \leq f_{esc}({\rm DB}) \leq 1.0$. For our calculations we assume $f_{\rm esc}(DB) = 0.6$, $f_{\rm esc}({\rm BL}) = 0.5 \times f_{\rm esc}(DB)$ and $f_{\rm esc}({\rm RB}) = 0.0$. In the LMC, we find a $L({\rm H}\alpha)$ weighted average H II $f_{\rm esc} \geq 0.41$ and $L_{\rm esc}({\rm H}\alpha) = 1.2 \times 10^{40}$ erg s^{-1}. In the SMC we find $f_{esc} \geq 0.44$ and $L_{esc}({\rm H}\alpha) = 1.9 \times 10^{39}$ erg s^{-1}. A small number of weakly ionized and/or shocked regions are excluded from our sample, because they show no clear structure in ratio images. These account for no more than 20 % of the total Hα emission and will not affect the results. Assuming all escaping radiation is absorbed in the WIM, Kennicutt et al. (1995) approximated $f_{\rm esc}$ using $L({\rm H}\alpha)_{\rm WIM}/L({\rm H}\alpha)_{\rm H\,II}$, and found values in the LMC and SMC between $25-35\%$ and $34-40\%$ respectively. These are similar to our $f_{\rm esc}$'s, and the idea that leaking photons from H II regions ionize the WIM (Haffner et al. 2009). Also, by correcting for $f_{\rm esc}$, we may more accurately derive the IMF of stellar populations from UV and Hα observations.

4 Results

To explore the link between local environment and $f_{\rm esc}$, we consider the H I column densities for all H II regions. The average LMC H I column in Figure 2a is half the SMC value, due in part to the projection of the flatter LMC compared to the irregular SMC. However, inclination will effect both RB and DB nebulae in the same way. Since a simple scaling can not bring the LMC H I distribution into agreement with the SMC, the distributions shown in (Fig. 2a) demonstrate a real difference between the LMC and SMC.

Independent of inclination, we find DB nebulae have lower values of N(H I) than RB nebulae in both galaxies. Figures 2b (LMC) and 2c (SMC) show the observed distribution in L(Hα) is bimodal. Without correcting for escaping radiation, we find the mean L(Hα) of DB H II regions to be $\approx$1 dex brighter than RB in the LMC, and 0.5 dex brighter in the SMC. In addition, we note the existence of objects with significant $f_{\rm esc}$ found near the outer regions of the SMC and LMC. The location of bright DB objects here may result in an unobstructed path for ionizing radiation to leave the galaxy.

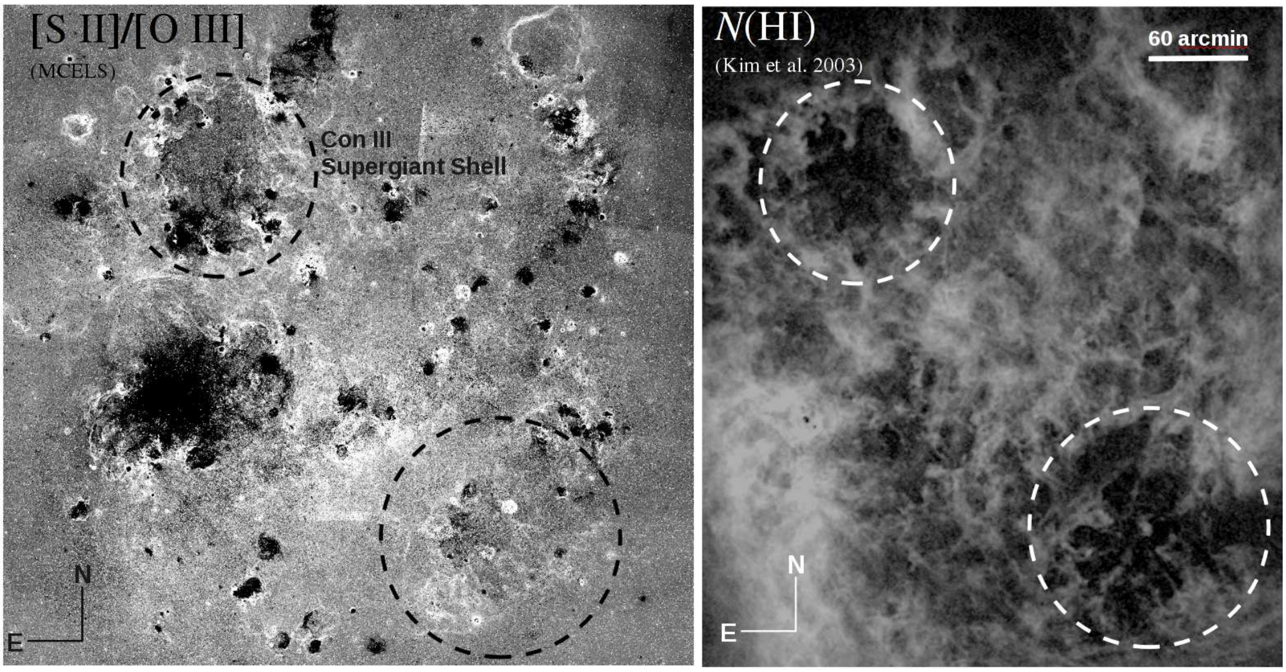

Figure 3: To the left is the ratio of [S II]/[O III] for the entire LMC galaxy. Black indicates lower ratios with a corresponding higher degree of ionization. The right is the H I column density map from Kim et al. (2003). Higher column densities are shown in white.

Figures 3 and 4 show striking differences in the large scale ionization and H I structures of the LMC and SMC. The LMC ISM is very filamentary and porous, with more highly ionized, low density bubbles surrounded by dense, weakly ionized shells. By contrast, the SMC ISM is more homogeneous, with less evidence of ionization gradients around localized ionization sources. Differences in Figures 2b and 2c are consistent with a scenario where massive star feedback and a higher star-formation rate has created a filamentary ISM in the LMC, allowing more radiation from lower luminosity nebulae to escape into the WIM and potentially out of the galaxy. However, both galaxies

Bulletin de la Société Royale des Sciences de Liège, Vol. 80, 2011, p. 410 - 414

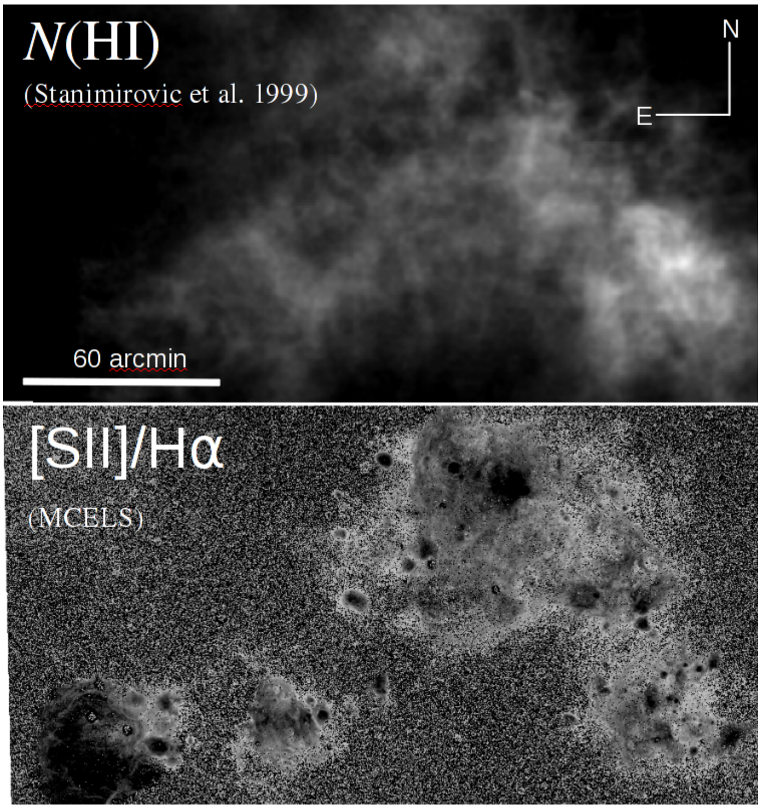

Figure 4: Similar to Figure 3, the top panel is the projected H I column density (Stanimirovic et al. 1999). Higher column densities are shown in white. The bottom panel shows the ratio of [S II]/Hα for the entire SMC. Black again indicates lower ratios with a corresponding higher degree of ionization.

have a similar escape fraction and further work is needed to understand the interplay between large scale structure and the escape fraction of ionizing radiation from H II regions.

Acknowledgements

This research is supported by NSF grant AST-0805476.

References

Ferland, G. J., Korista, K. T., Verner, D. A., Ferguson, J. W., Kingdon, J. B., & Verner, E. M., 1998, PASP, 110, 761

Giammanco, C., Beckman, J. E., Zurita, A., & Relaño, M. 2004, A&A, 424, 877

Haffner, L.M., Dettmar, R.J., Beckman, J.E., et al., 2009, RvMP, 81, 969

Kennicutt R.C., Bresolin, F., Bomans, D.J., Bothun, G.D., Thompson, I.B., 1995, AJ, 109, 594

Kim, S., Staveley-Smith, L., Dopita, M.A. Sault, R.J. Freeman, K.C., Lee, Y., Chu, Y.H., 2003, ApJS, 148, 473

Smith, R.C., Points. S.D., Chu, Y.H., Winkler, P.F., Augilera, C., Leiton, R., & the MCELS Team, 2005, AAS, 207, 2507

Sokasian, A., Abel, T., & Hernquist, L. 2003, MNRAS, 340, 473

Stanimirovic, S., Stavely-Smith, L., Dickey, J.M., Sault, R.J. & Snowden, S.L., 1999, MNRAS, 302, 417